Atomic and electronic structures of the lattice mismatched metal–ceramic interface

2004 J. Phys.: Condens. Matter 16 5781

(http://iopscience.iop.org/0953-8984/16/32/014)

INSTITUTE OF PHYSICS PUBLISHING JOURNAL OF PHYSICS: CONDENSED MATTER

J. Phys.: Condens. Matter **16** (2004) 5781–5790 PII: S0953-8984(04)79119-5

Atomic and electronic structures of the lattice mismatched metal–ceramic interface

L M Liu[1], **S Q Wang and H Q Ye**

Shenyang National Laboratory for Materials Science, Institute of Metal Research, Chinese Academy of Sciences, Shenyang 110016, People's Republic of China

E-mail: lmliu@imr.ac.cn

Received 13 April 2004
Published 30 July 2004
Online at stacks.iop.org/JPhysCM/16/5781
doi:10.1088/0953-8984/16/32/014

Abstract

This research purposes to investigate the atomic and electronic structures of the Al/TiC(001) interface with lattice misfit using the *ab initio* pseudopotential approach. A detailed analysis of the relaxed atomic structure reveals that the atoms over the initial unfavourable sites relax to the favourable sites along the lateral plane. The properties of the semicoherent interface can be taken as averages over the different coherent sites. In addition, the interface atoms in relatively favourable regions are dragged near to the interface, while those in unfavourable regions are pushed away from the interface. Therefore, a large warping near the interface is made perpendicular to the lateral plane. The calculated adhesions explain the different wetting results from the viewpoint of structural transition. The subsequent analysis of electronic properties demonstrates that adhesions dominate mainly via the strong Al–C covalent bond.

(Some figures in this article are in colour only in the electronic version)

1. Introduction

Metal–ceramic interfaces are widely used in a large number of industrial applications, such as in microelectronic devices, heterogeneous catalysis, corrosion protection, and metal–matrix composites [1–3]. In all these applications, the interfacial structure and adhesion can have significant effects on their performances, so the interfaces between the ceramic and substrate metal or matrix are rather important. But the factors which control the interfacial properties have not been fully examined. Therefore, it is highly desirable to achieve a better understanding of the metal–ceramic interface at the atomic level.

[1] Author to whom any correspondence should be addressed.

Due to its high melting point and hardness, TiC is widely used in coating and cutting materials. Experimentally, several groups of researchers have fabricated and investigated metal–titanium carbide materials. Some groups of researchers [4, 5] showed that Al/TiC had a rather high contact angle and low adhesion energy and this led them to the conclusion that Al did not wet the TiC. But some other groups of researchers [6, 7] demonstrated that Al could wet TiC at high temperature. The different experiments give conflicting answers to the primary question of whether Al wets TiC or not.

Many first-principles density functional theory (DFT) calculations have been carried out for metal–ceramic interfaces. However, most of them are confined to metal–oxide interfaces [8–20]. The metal–transition metal carbide interfaces are not widely explored [21–28]. In addition, most of these studies are confined to well lattice matched interfaces. Although the lattice misfit substantially influences the adhesions and mechanical properties of heterointerfaces [29–31], only a few lattice mismatched interfaces have been examined. Benedek and co-workers [32, 33] studied the polar MgO{222}/Cu interface and found that the interface electronic structure varied appreciably with the local environment. Dudiy and Lundqvist [34] studied Co/TiC(N)(001) interfaces, and their results showed that the dominant bonding of the interface was the strong covalent bond between the Co 3d and C(N) 2p orbitals, and the calculated adhesion strength was consistent with the wetting experiments. Recently, Christensen and Carter examined the ZrO_2/Ni(111) interface [35], and they found that ZrO_2 adhered strongly at the monolayer level but thicker ceramic films interacted weakly with Ni substrate.

The Al/TiC(001) interface, with a lattice mismatch of 6.7% between the larger TiC and the Al, is known to be semicoherent. Due to the relatively large misfit, there exist misfit dislocation networks, and there are coherent regions between these dislocation networks. As a preliminary step toward understanding the semicoherent interface system, the coherent regions have been examined making the coherent approximation in our previous study [36]. To understand better the misfit regions, we use a more realistic model to study the bonding of the interface in this study.

One main purpose in this work is to investigate the correlation between the adhesion and atomic or electronic structures of the metal–transition metal ceramic interface by means of density functional theory. A further purpose is to explore the intrinsic relationship between coherent regions and semicoherent regions in order to shed some light upon the misfit interface.

2. Methodology

We utilize the Dacapo [37] package in our calculations, based on density functional theory [38, 39]; it uses a plane-wave (PW) basis set for the expansion of the single-particle Kohn–Sham wavefunctions and Vanderbilt ultrasoft pseudopotentials (US PP) [40] to describe ionic cores. The exchange–correlation energy is described using the generalized gradient approximation of Perdew and Wang (GGA-PW91) [41]. The self-consistent PW91 density is determined by iterative diagonalization of the Kohn–Sham Hamiltonian, coupled with a Pulay mixing scheme [42]. A Fermi function is used with a temperature broadening parameter of 0.2 eV to improve convergence. Ground-state atomic geometries are determined by minimizing the Hellmann–Feynman forces. The interface geometries and the isolated slabs were optimized via minimization of the atomic forces to a tolerance of 0.1 eV $Å^{-1}$ except where the specific tolerance is given below. The Brillouin zone is sampled with a Monkhorst–Pack k-point grid [43]. For the slab a $4 \times 4 \times 1k$-point mesh is used. The plane-wave cut-off in our calculations is 350 eV. This set of parameters ensures a total energy convergence of 0.01 eV per atom. In our previous study [36], the pseudopotentials for both bulk TiN and Al were

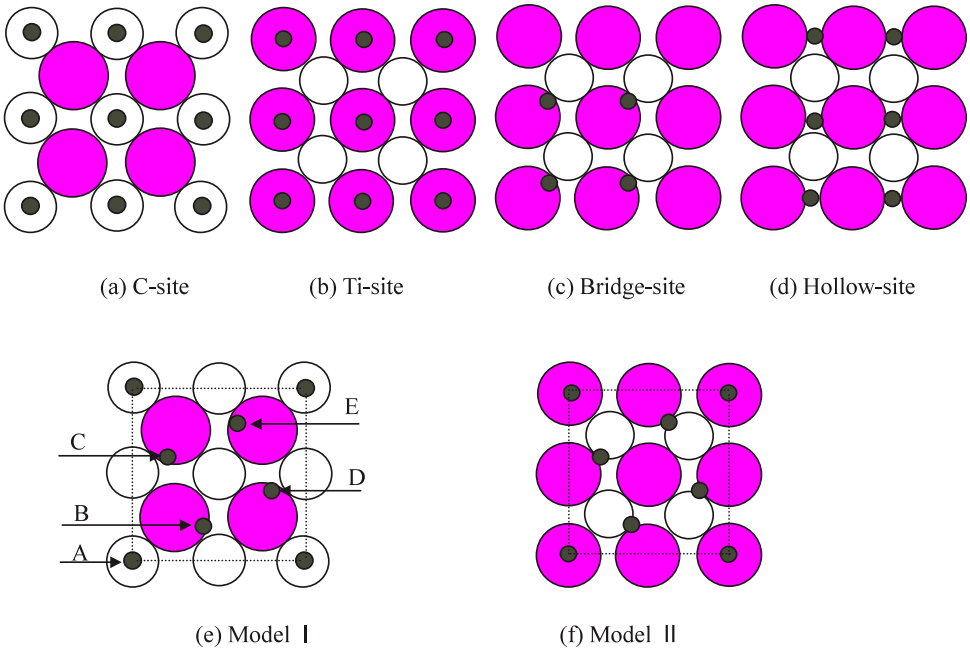

Figure 1. Six interface configurations for the Al/TiC(001) interfaces. Parts (a)–(d) show the coherent model. Parts (e) and (f) show the semicoherent model. The small spheres represent the Al atoms; the medium-sized spheres represent the C atoms; the large spheres represent the Ti atoms. The different Al atoms of the semicoherent model have been labelled as A–E in part (e).

fully tested and showed good agreement with other calculations and experiments. The same pseudopotentials are used in this study.

3. Interfaces

3.1. Model geometry

To identify the optimal interface geometry we consider different stacking sequences, placing the interfacial Al over different positions with respect to the TiC surface lattice structure, as shown in figure 1. For the coherent interface, we examine the hollow site. The parameters and models are the same as in the previous study of other sites (Ti sites, C sites, and bridge sites) [36]. For the semicoherent interface model, we use a superlattice geometry in which a four-layer slab of Al(001) is placed on a four-layer TiC(001) slab. The free surfaces of Al and TiC are separated by at least 10 Å of vacuum. We consider two possible structures: the original Al above the C atom (model I) and the original Al above the Ti atoms (model II). Model I and model II are shown in figures 1(e) and (f), respectively. For such a semicoherent model, there is a modest lattice mismatch of 4.8%.

3.2. Work of adhesion

The ideal work of adhesion, W_{ad}, an important fundamental quantity for predicting the mechanical properties, is defined as the reversible work needed to separate an interface into two free surfaces [1]. W_{ad} can be calculated as the difference in total energy between the

Table 1. The calculated relaxed work of adhesion (W_{ad}) and the interfacial separation (d_0) for the Al/TiC interface systems.

Systems	Stacking	d_0 (Å)	W_{ad} (J m^{-2})
Semicoherent	Model I	2.13	1.39
	Model II	2.34	1.92
Coherent	Ti site	2.70	0.51[a]
	C site	2.08	2.63[a]
	Bridge site	2.29	1.44[a]
	Hollow site	2.19	1.79
Experiment			0.485 (700 °C)[b]
			1.32 (800 °C)[c]
			1.41 (900 °C)[c]
			1.61 (1000 °C)[c]

[a] Reference [36].
[b] References [4, 5].
[c] Reference [6].

interface and its isolated slabs:

$$W_{ad} = (E_A^{tot} + E_B^{tot} - E_{A/B}^{tot})/S. \quad (1)$$

Here, E_A^{tot} and E_B^{tot} are the total energy of the relaxed, isolated TiC and Al slabs in the same supercell when one of the slabs is retained and the other one is replaced by a vacuum, respectively. $E_{A/B}^{tot}$ is the total energy of the Al/TiC interface system. S is the total interface area of the unit cell.

Our calculated results on the optimal interfacial separation (d_0) and work of adhesion (W_{ad}) for all interface structures are shown in table 1. For the coherent interface, we note that the C site is the most favourable site, the hollow site is the second most favourable one, the bridge site is the third most favourable one, and the Ti site is the most unfavourable site of the four possible sites.

For the semicoherent interface, the interface of model II exhibits the larger W_{ad} value of 1.92 J m^{-2}, and the interface of model I has a little lower W_{ad}, 1.39 J m^{-2}. The mean interface separation of model I is about 2.13 Å. This is just between the C site and bridge site values for the coherent interface. The mean interface separation of model II is 2.34 Å, which is even larger than that of model I. Subsequent structure analysis will clarify this issue.

The experimental phenomena show that the wetting of Al/TiC is dynamic with increasing temperature. At low temperature, the wetting angle is rather high, and the interface is non-wetting. This situation may correspond to the unfavourable structure. With increase of temperature, the interface suddenly begins to wet, and gradually becomes more wetting. Interestingly, the experimental adhesion at low temperature (700 °C) is in good agreement with the value for the Ti site of the coherent interface. The experimental result for medium temperature (800–900 °C) is quantitatively consistent with the calculated result for model I. The wetting result for high temperature (1000 °C) is very close to W_{ad} for model II. Subsequent structure analysis will reveal that the reason that model II has larger adhesion is correlated with the stronger Al–C bonding of the C site. This is consistent with experimental results, which showed that the change of wetting angle was related to the formation of Al_4C_3 at high temperature [6, 7].

Our results exhibit the same trend as those from the experiments. Therefore, the process of wetting may be a result of a structural transition from the unfavourable case to the favourable one. At low temperature, the structure is more correlated with the Ti site. With increasing

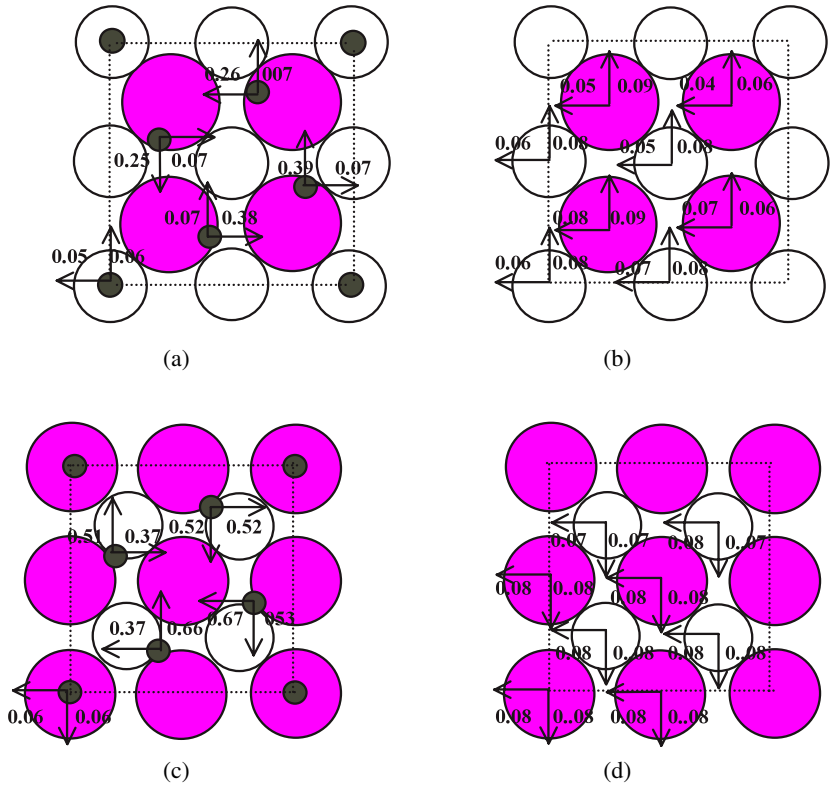

Figure 2. The displacements of the interface atoms. The arrows indicate the direction of in-plane displacements, and the magnitude is given on the right. The unit is Å. Parts (a) and (c) show the movements of the Al atoms for model I and model II, respectively. Parts (b) and (d) show the movements of the Ti and C atoms for model I and model II, respectively.

temperature, the structure gradually begins to be more correlated with the C site. So our results may quantitatively explain the conflicting experimental results from the viewpoint of a structural transition.

3.3. Interface structure

3.3.1. Lateral movement of interfacial atoms. To understand how the semicoherent interface reaches its stable structure, it is necessary to find how the favourable and unfavourable atoms move along the lateral plane.

Figure 2 shows the lateral displacements of interfacial layer atoms. First, the two different models exhibit some common features. For the ceramic slab side, the movements of Ti and C atoms are in nearly the same direction and of nearly the same magnitude. That is to say, the relative movements of the Ti and C atoms are rather small. For the Al slab side, the atomic displacements exhibit significantly different directions and magnitudes. In addition, the movements are also larger than those in the ceramic case.

On the other hand, the atoms in the different semicoherent models obey different displacement rules. For model I, the Al atoms over the bridge site move to the more favourable hollow site, while the Al atom over the C site, the most favourable site, shows a very small movement. For model II, the Al atoms over the bridge site relax close to the C site, while the Al atom over the Ti site stays in its unfavourable place. Subsequent analysis of layer warping

Table 2. The lengths of the Al–C and Al–Ti bonds of the interface layer atoms for model I and model II. The atom labelling A–E relates to figure 1(e).

Al atoms	Al–C bond (Å)		Al–Ti bond (Å)	
	Model I	Model II	Model I	Model II
A	2.00	3.82	3.05	3.22
B	2.24	2.01	2.65	2.93
C	2.38	2.01	2.62	2.92
D	2.40	2.01	2.62	2.93
E	2.31	2.01	2.58	2.93

will show that the Al atom over the Ti site has been separated by nearly 1.13 Å from its plane, and it has a weak interaction with the Ti atom.

Since the structures of semicoherent interfaces consist of the different sites of the four coherent sites, it is reasonable to take the semicoherent interface as the average of the symmetric coherent interfaces, as discussed in other studies [33]. For model I, the initial configuration mainly consists of one C site and four bridge sites, and the final structure can be seen to consist of one C site and four hollow sites. For model II, the initial configuration consists of one Ti site and four bridge sites, and the final structure is close to four C sites and one Ti site. Overall, the final structure of model II is more correlated with the C site than that of model I.

3.3.2. Bond lengths of interfacial atoms. In fact, the atoms of interfacial layers will not only adjust their places along the lateral plane, but also optimize their bonding across the interface. The results for the relaxed lengths of the Al–C and Al–Ti bonds across the interface are shown in table 2.

For model I, the atoms can be separated into two groups according to the lengths of the Al–C or Al–Ti bond. One group is atoms A (as labelled in figure 1). The bond length of the Al–C bond is 2.00 Å, and the length of the Al–Ti bond is 3.05 Å. The length of the Al–C bond is even shorter than that for the C site of the coherent interface, 2.09 Å. This results from the strong interaction between Al and C atoms. The other group is atoms B–E (as labelled in figure 1). Although each atom of this group sits just over the centre of around four atoms (hollow site), the lengths of the Al–C bonds are a little shorter than that of the Al–Ti bond. The reason is that the strong interaction of the Al–C bond draws the C atom nearer to the Al atom. In addition, the length of each Al–Ti bond is shorter than that for bulk TiAl (2.82 Å), so the Al–Ti bond should also have some effect on the adhesion.

For model II, the atoms can also be separated into two groups according to the lengths of the Al–C or Al–Ti bond. One group is atoms A, corresponding to the Ti sites of the coherent interface. The atom distance (3.82 Å) between the Al and C atoms is so large that there is almost no interaction between them. The length of the Al–Ti bond is 3.22 Å, which is also rather large. The other group is atoms B–E. The length of each Al–C bond is 2.01 Å. The lengths of the Al–Ti bonds are in the range of 2.92–2.93 Å. The length of each Al–C bond of this group is rather close to that of the shorter one of model I (atom A). In addition, the length of each Al–C bond is evidently shorter than that of the longer bond group of model I (atoms B–E). Meanwhile, the length of each Al–Ti bond is longer than the corresponding one in model I.

Overall, most of the Al–C bonds of model II are shorter than those of model I. In addition, the length of each Al–Ti bond of model I is shorter than the corresponding one for model II. It is evident that the Al–Ti bond of model I has more effect on the adhesion than that of model II.

Table 3. Layer warping along the interface for model I and model II. The interfacial layers of the TiC (Al) slab are denoted as TiC1 (Al1). The layer nearest to the interface TiC (Al) slab is denoted as TiC2 (Al2), etc.

	Layer warping (Å)	
Interlayer	Model I	Model II
Al4	0.004	0.006
Al3	0.024	0.017
Al2	0.121	0.820
Al1	0.141	1.136
TiC1	0.227	0.114
TiC2	0.033	0.031
TiC3	0.012	0.021
TiC4	0.119	0.116

So the main reason that the adhesion of model II is stronger than that of model I is the higher strength of the Al–C bond.

3.3.3. Layer warping. The relaxed interfacial Al atoms are over different sites, favourable or unfavourable. The interfacial atoms will relax to appropriate distances from other atoms perpendicular to the interface.

Table 3 shows that the layer warping along the semicoherent interface. We note that model I and model II have one common feature. The warping of the ceramic side is confined to the vicinity of interface and surface and the warping of other layers can be neglected, while the warping of the metal side has extended to the second layer. The reason is that TiC has a larger elastic modulus than Al.

On the other hand, there are some different behaviours for the two semicoherent models. For the ceramic side, the warping of model I is a little larger than the coherent result. The main reason is that the Al atom over the C site greatly drags the C atom and takes the C atom out of its original plane. For model II, the warping of the ceramic side is a little smaller but comparable to result for the C site obtained for the coherent interface. The reason is that the final configuration of model II is quite close to that of the C site of the coherent interface.

Next, for the Al slab side, the warping of model II is rather larger than that of model I. The reason is that the Al atom of model II over the Ti site is rather unfavourable, and it is repelled to 1.13 Å away from the original layer. This is the main reason that model II has even larger interface separation than model I.

Overall, in the favourable regions, the interfacial atoms of both sides drag towards each other. In the unfavourable regions, the atoms of both sides repel each other. So the interfacial atoms of both sides have some warping, as found in previous coherent studies.

3.4. Electronic structure and bonding

In addition to the atomic structure and interfacial adhesion, the interfacial electronic structure plays an important role in determining the interfacial properties. To reveal the bonding nature, we analyse the atom-projected density of states (DOS) for the interfacial layers. As found in the structure analysis, the interfacial Al, C and Ti atoms are separated into groups according to their final sites. For model I, atom A is over the C site, and all other atoms are over the hollow sites. For model II, atom A is over the Ti site, and all other atoms are over the C sites. Because the electronic properties of members of the same group are rather alike, only one representative atom-projected DOS for each group is shown in figure 3.

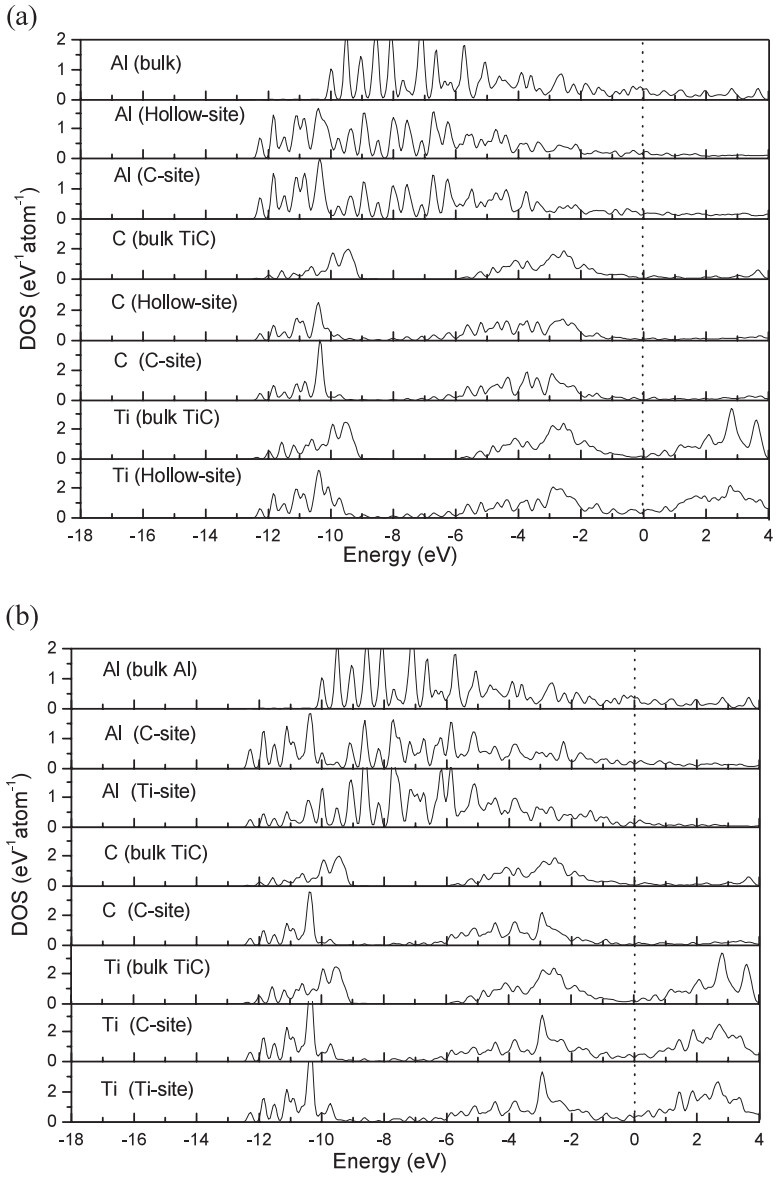

Figure 3. The atom-projected DOS for model I (a) and model II (b) interface structure. Al(bulk) shows the bulk Al atom-projected DOS. C(bulk TiC) shows the C atom-projected DOS of bulk TiC. C(C site) shows the interfacial C over the C site atom-projected DOS, etc. The vertical dotted line gives the location of the Fermi energy.

First, let us discuss the atom-projected DOS of model I. For both the C site and the hollow site, the DOS of the Al atoms shows a set of new low-energy states from −12 to −10 eV. In addition, the DOS of the interfacial Ti and C atoms moves slightly to the low-energy states. So the Al and TiC share the new states and have a common new peak around −11.5 eV. These new states make the TiC and Al bonding states with larger overlap, which contributes to the hybridization of Al 3sp–C 2sp and Al 3sp–Ti 3d orbitals to form the covalent bonds.

There is evidently a difference between the C site and the bridge site. First, the Al atom-projected DOS of the C site has an evidently stronger and narrower peak at about −10.5 eV than that of the bridge site. This new peak just corresponds to the peak of the C atom-projected DOS of the C site. Second, the Al atom-projected DOS of the C site from −10 to −7 eV, which is just the energy band gap of bulk TiC, is weaker than that of the hollow site. Overall, the Al–C bond of the C site is stronger and more localized than that of the hollow site.

Next, let us concentrate on the atom-projected DOS of model II. For the C site, the Al atom-projected DOS also shows new states from −12 to −10 eV, which is similar to the case for the C site of model I. So the Al–C and Al–Ti bonds are also strong covalent bonds. For the Ti site, the Al atom-projected DOS looks like that of the bulk Al, as found for the coherent Ti site in our previous study. So the Al–Ti interaction should be a metallic bond.

Overall, the interface adhesion is correlated with the Al–C and Al–Ti covalent bonds. As discussed in the analysis of bond lengths, the Al–C bond plays a more important role. In addition, the Al–C bond of the C site is substantially stronger than those for other sites. So the final structure with more C sites has larger adhesion. This explains why model II has larger adhesion energy.

4. Summary and conclusions

In this work, first-principles calculations are performed for the relatively large misfit Al/TiC(001) interface using relatively modest misfit models. The atomic structures, electronic properties, and adhesion of semicoherent regions have been thoroughly investigated. The relationship between the semicoherent and coherent regions is also discussed.

Some interesting phenomena are found in the relaxation of the Al slab. First, the atoms over the unfavourable sites adjust their initial positions along the lateral plane to find more favourable sites. Second, the interfacial atoms in relatively favourable regions are dragged nearer to the interface, while those in unfavourable regions are pushed away from the interface. This leads to a large warping at interface layer.

An analysis of the relaxed atomic structure reveals that the favourable structure consists of four C sites and one Ti site, and the unfavourable model is made up of one C site and four hollow sites. It is reasonable to take the adhesion of the semicoherent interface as the average over the different coherent sites, as in other studies. The different wetting results are explained from the viewpoint of the structural transition with temperature change.

Through analysis of the electronic structure, we find that the main mechanism of the interface adhesion is the strong Al–C covalent bonding. Meanwhile, we reveal that the Al–C bonding of the C site is substantially stronger than that for other sites. This is the primary reason that the final structure, with more C sites, has larger adhesion.

Acknowledgments

The authors are grateful to Dr Asbjorn Christensen for fruitful discussions and kind help. This work was supported by the Special Funds for Major State Basic Research Projects of China (No G2000067104).

References

[1] Finnis M W 1996 *J. Phys.: Condens. Matter* **8** 5811
[2] Christensen A, Jarvis E A A and Carter E A 2001 *Chemical Dynamic in Extreme Environment* ed R A Dreeler (Singapore: World Scientific) p 490

[3] Sinnott S B and Dichey E C 2003 *Mater. Sci. Eng.* R **43** 1
[4] Samsonov G M and Vinitskii I M 1980 *Handbook of Refractory Compounds* (New York: IFI Plenum) p 217
[5] Kosolapova T Ya 1990 *Handbook of High Temperature Compounds: Properties, Production and Application* (New York: Hemisphere) p 685
[6] Contreras A, León C A, Drew R A L and Bedolla E 2003 *Scr. Mater.* **48** 1625
[7] Aguilar E A, León C A, Contreras A, López V H, Drew R A L and Bedolla E 2002 *Composites* A **33** 1425
[8] Li C, Wu R, Freeman A J and Fu C L 1993 *Phys. Rev.* B **48** 8317
[9] Bogicevic A and Jennison D R 1999 *Phys. Rev. Lett.* **82** 799
[10] Christensen A and Carter E A 2000 *Phys. Rev.* B **62** 16968
[11] Zhang W and Smith J R 2000 *Phys. Rev. Lett.* **85** 3225
[12] Zhukovskii Y F, Kotomin E A, Jacobs P W M and Stoneham A M 2000 *Phys. Rev. Lett.* **84** 1256
[13] Batyrev I G, Alavi A and Finnis M W 2000 *Phys. Rev.* B **62** 4698
[14] Wang X G, Chaka A and Scheffler M 2000 *Phys. Rev. Lett.* **84** 3650
[15] Łodziana Z and Nørskov J K 2001 *J. Chem. Phys.* **115** 11261
[16] Javis E A, Christensen A and Carter E A 2001 *Surf. Sci.* **487** 55
[17] Wang X G, Smith J R and Evans A 2002 *Phys. Rev. Lett.* **89** 286102
[18] Siegel D J, Hector L G Jr and Adams J B 2002 *Phys. Rev.* B **65** 085415
[19] Javis E A and Carter E A 2003 *J. Am. Ceram. Soc.* **86** 373
[20] Yang Z, Wu R, Zhang Q and Goodman D W 2002 *Phys. Rev.* B **65** 155407
[21] Hoekstra J and Kohyama M 1998 *Phys. Rev.* B **57** 2334
[22] Profeta G, Continenza A and Freeman A J 2001 *Phys. Rev.* B **64** 45303
[23] Dudiy S V, Hartford J and Lundqvist B I 2000 *Phys. Rev. Lett.* **85** 1898
[24] Siegel D J, Hector L G Jr and Adams J B 2002 *Surf. Sci.* **498** 321
[25] Siegel D J, Hector L G Jr and Adams J B 2002 *Acta. Mater.* **50** 619
[26] Arya A and Carter E A 2003 *J. Chem. Phys.* **118** 8982
[27] Liu L M, Wang S Q and Ye H Q 2003 *J. Phys.: Condens. Matter* **15** 8103
[28] Liu L M, Wang S Q and Ye H Q 2003 *Surf. Interface Anal.* **35** 835
[29] Hong T, Smith J R and Srolovitz D J 1995 *Acta Metall. Mater.* **43** 2721
[30] Schnitker J and Srolovitz D J 1998 *Modelling Simul. Mater. Sci. Eng.* **6** 153
[31] Benedek R, Seidman D N and Woodward C 2002 *J. Phys.: Condens. Matter* **14** 2877
[32] Benedek R, Seidman D N, Minkoff M, Yang L H and Alavi A 1999 *Phys. Rev.* B **60** 16094
[33] Benedek R, Alavi A, Seidman D N, Yang L H, Muller D A and Woodward C 2000 *Phys. Rev. Lett.* **84** 3362
[34] Dudiy S V and Lundqvist B I 2001 *Phys. Rev.* B **64** 045403
[35] Christensen A and Carter E A 2001 *J. Chem. Phys.* **114** 5816
[36] Liu L M, Wang S Q and Ye H Q 2004 *Surf. Sci.* **550** 835
[37] Hansen L *et al*, *Dacapo-1.30* Centre for Atomic Scale Materials Physics (CAMP), Denmark Technical University
[38] Hohenberg P and Kohn W 1964 *Phys. Rev.* **136** B864
[39] Kohn W and Sham L J 1965 *Phys. Rev.* **140** A1133
[40] Vanderbilt D 1990 *Phys. Rev.* B **41** 7892
[41] Perdew J P, Chevary J A, Vosko S H, Jackson K A, Pederson M A, Singh D J and Fiolhais C 1992 *Phys. Rev.* B **46** 6671
[42] Kresse G and Forthmüller J 1995 *Comput. Mater. Sci.* **6** 15
[43] Monkhorst H J and Pack J D 1976 *Phys. Rev.* B **13** 5188